Supplementary Materials

Microfluidic synthesis and accurate immobilization of low-density QDs encoded magnetic microbeads for multiplex immunoassay

Zhou Sha [a], Tianyi Ling [a], Wenqi Yang [a], Haosu Xie [a], Chunnan Wang [a], Shuqing Sun [a, *]

[a] Institute of Biopharmaceutical and Healthcare Engineering, Shenzhen International Graduate School, Tsinghua University, Shenzhen 518055, China

* Prof. Shuqing Sun: Institute of Biopharmaceutical and Healthcare Engineering, Shenzhen International Graduate School, Tsinghua University, Shenzhen 518055, China

Email: sun.shuqing@sz.tsinghua.edu.cn

Tel: +86-(0)755-2603 6026

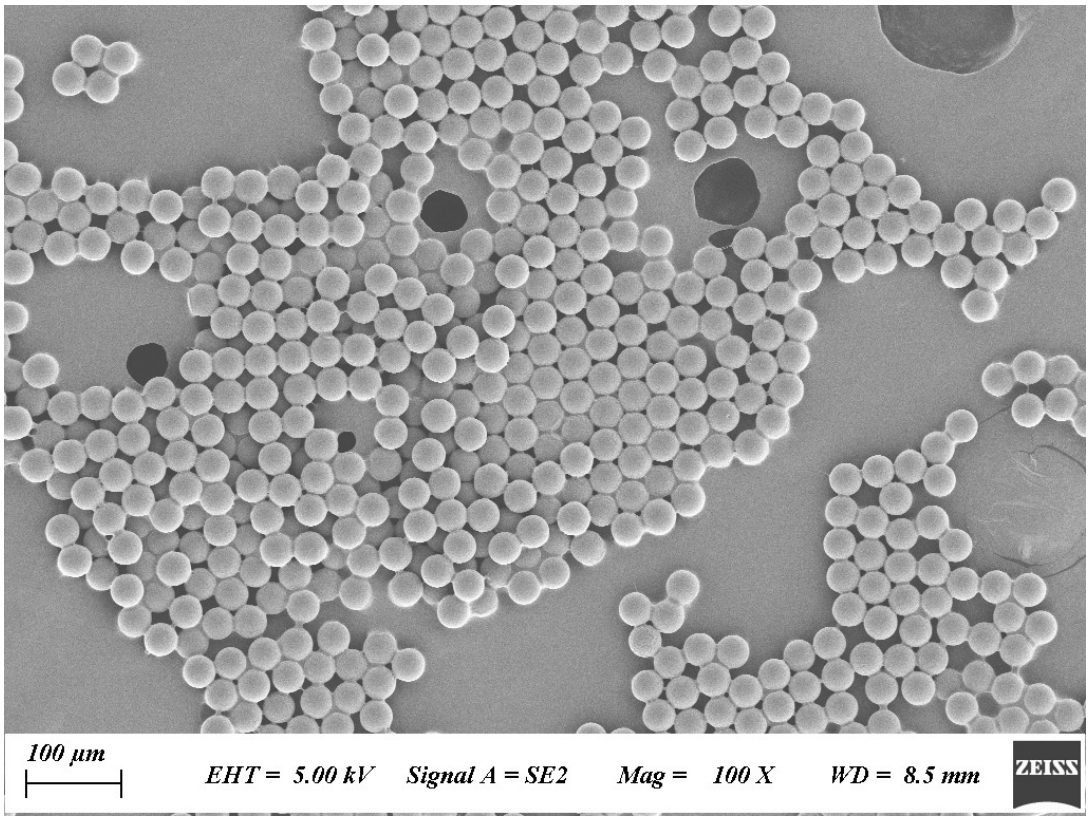

Figure S1a. SEM image of QDs encoded magnetic microbeads

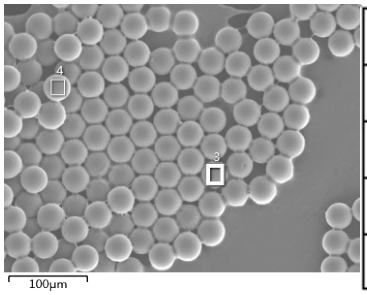

Element	Atom percent
C	84.82
O	14.94
Fe	0.23
Total amount	100.00

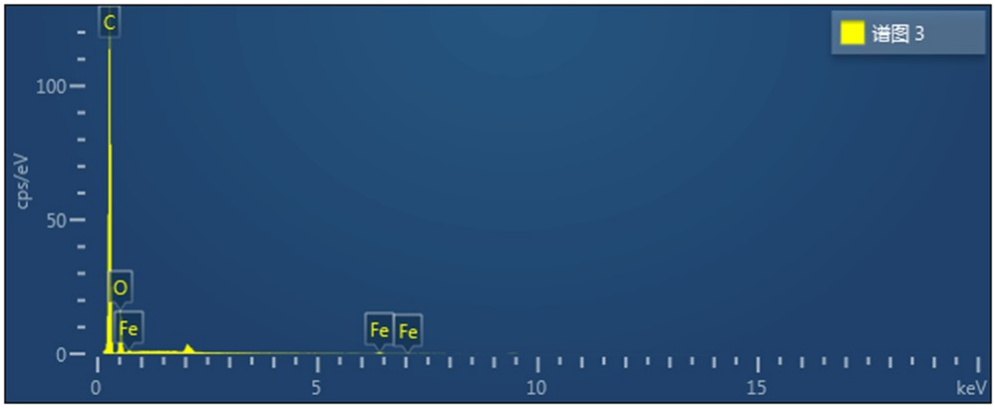

Figure S1b. EDX mapping of QDs encoded magnetic microbeads

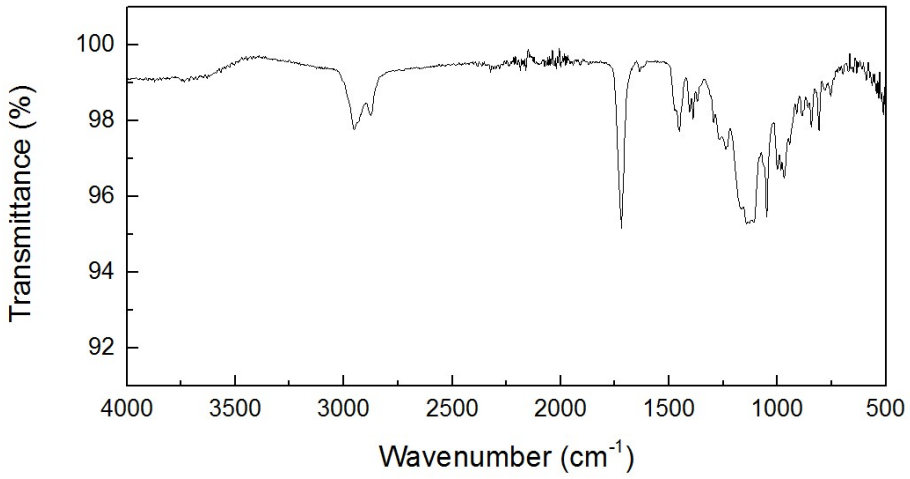

Figure S2a. Fourier transform infrared (FTIR) spectroscopy of IBOMA and ETPTA copolymer.

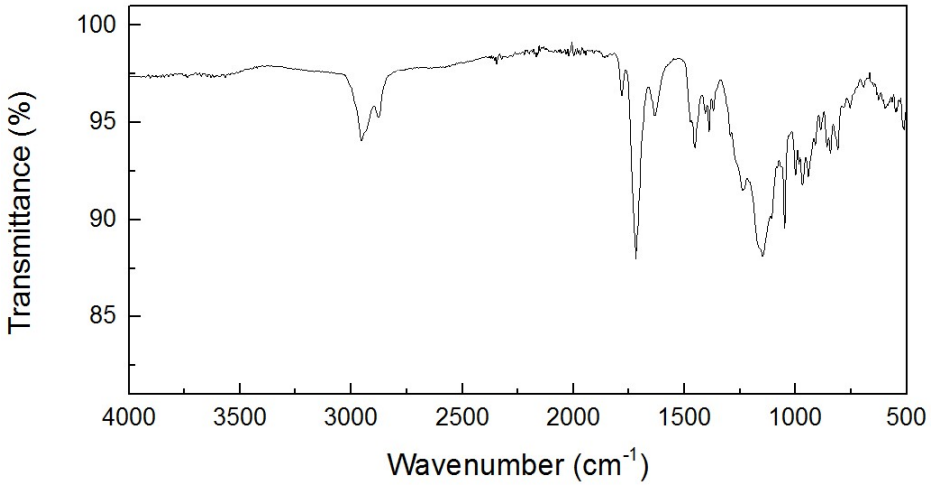

Figure S2b. Fourier transform infrared (FTIR) spectroscopy of IBOMA, ETPTA and MA copolymer before the hydrolysis of anhydride groups.

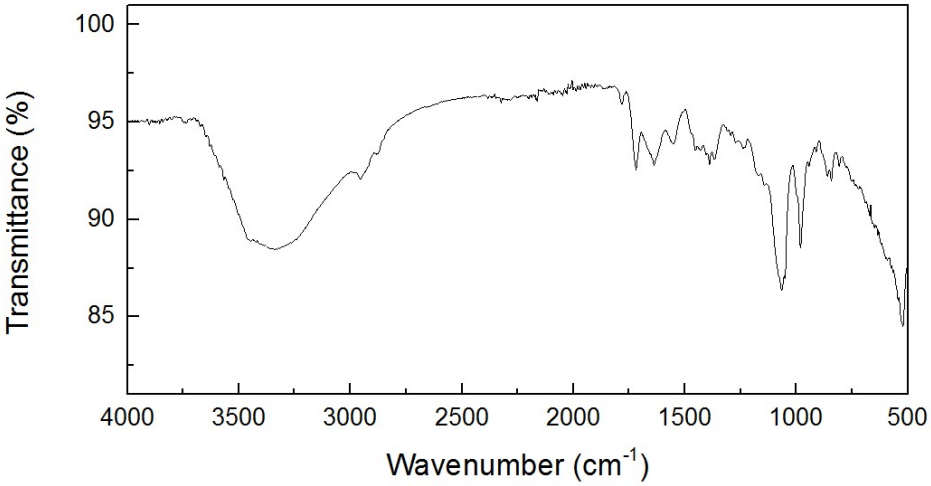

Figure S2c. Fourier transform infrared (FTIR) spectroscopy of IBOMA, ETPTA and MA copolymer after the hydrolysis of anhydride groups.

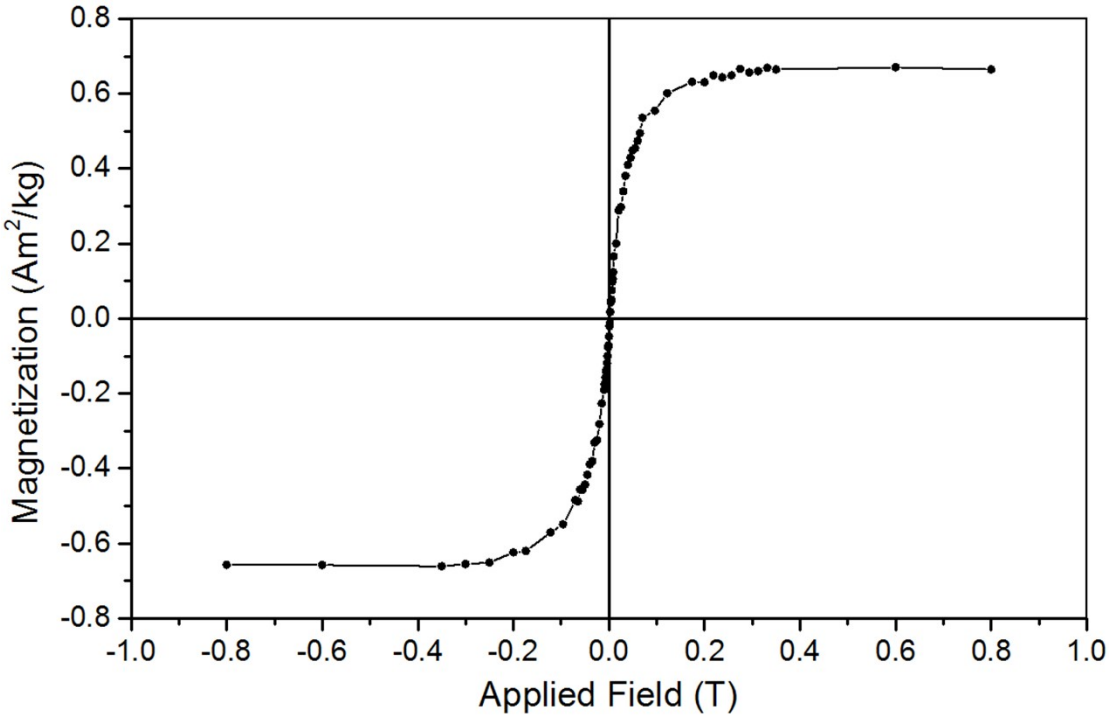

Figure S3. Magnetization curve (T = 300 K) of dried microbeads prepared in this work.

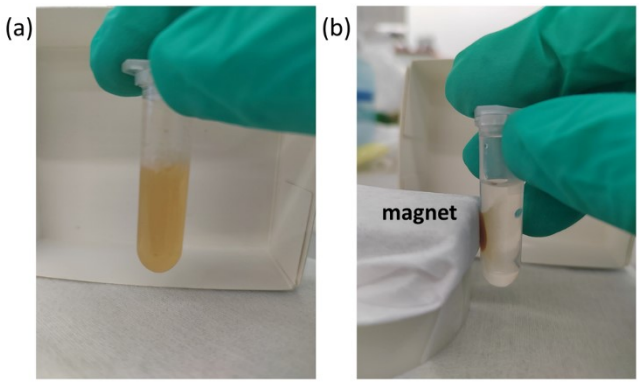

Figure S4. Performance of magnetism. (a) Microbeads were dispersed in the solution. (b) Microbeads aggregated under magnetic force.

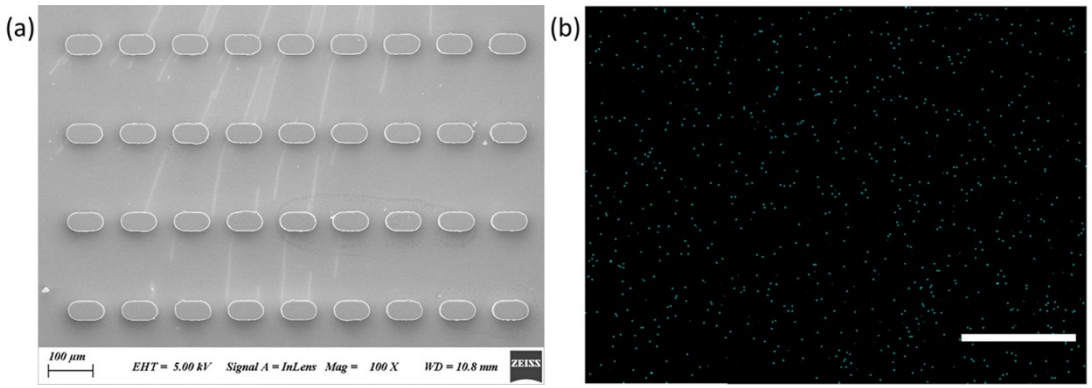

Figure S5. (a) SEM image of patterns without filling nickel powder. (b) EDS analysis of Nickel elements (blue points) in Fig S5a. The scale bar was 250 µm.

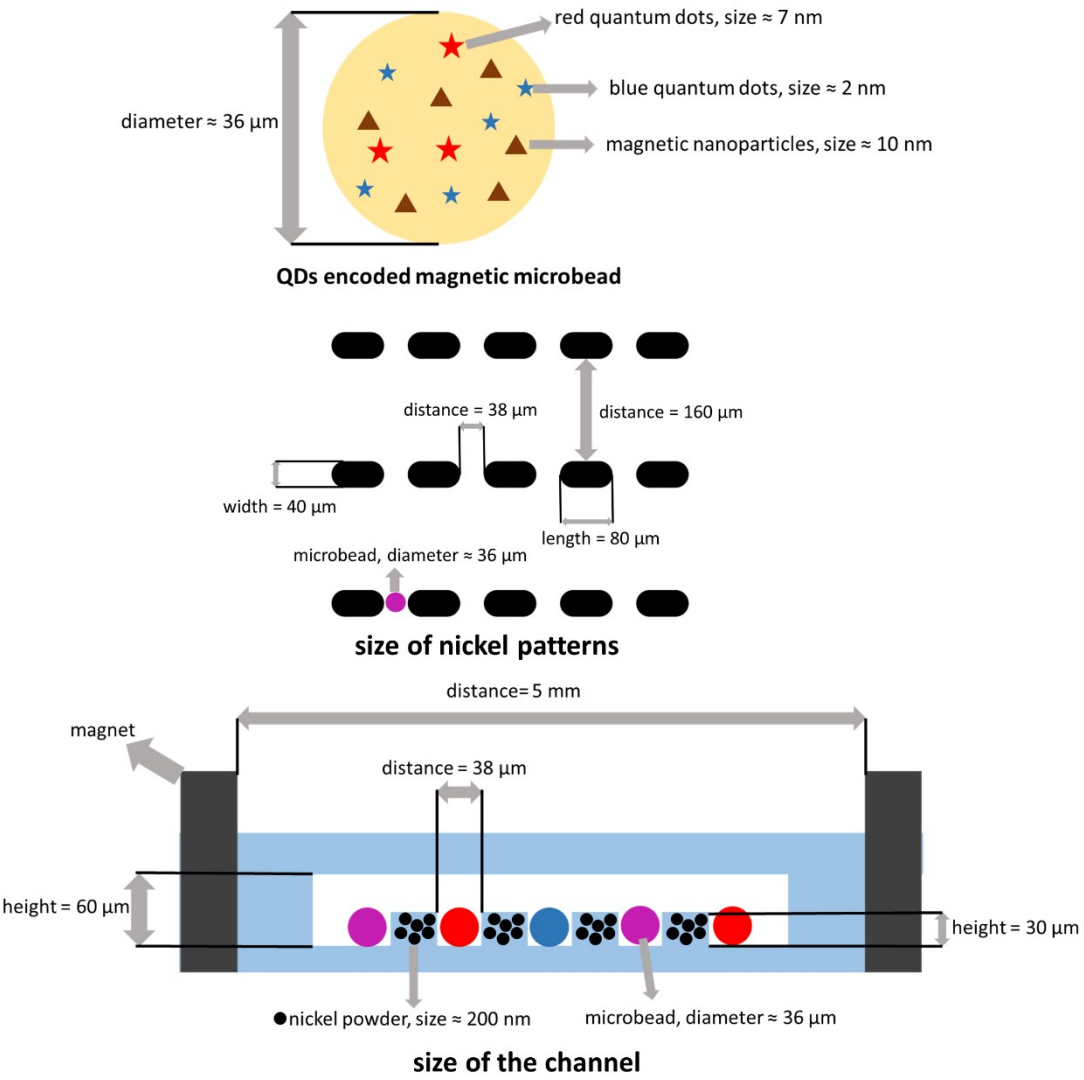

Figure S6. Sizes of microbeads, nickel patterns and the channel.

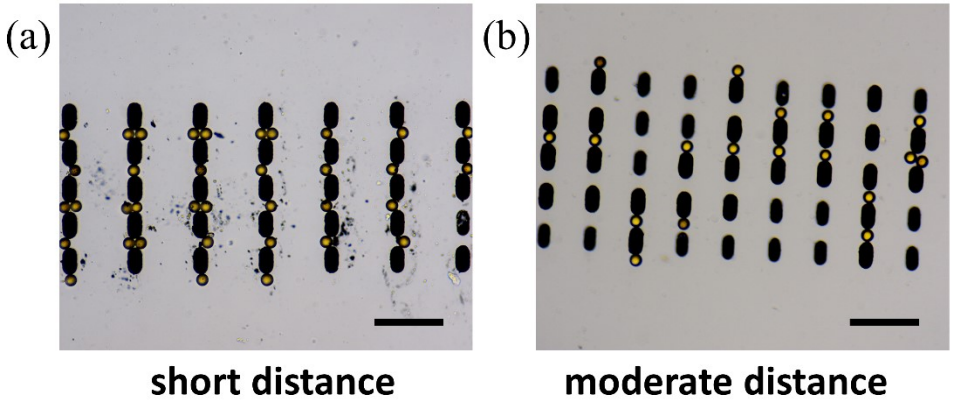

Figure S7. Influence of distance between nickel patterns on the trapping rate of microbeads. Distance in (a) was about 30 µm, distance in (b) was about 35 µm.

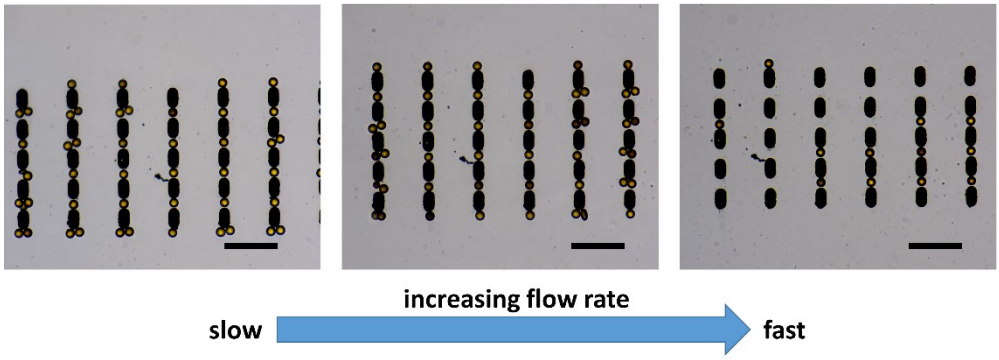

Figure S8. Influence of flow rate on the trapping rate of microbeads.

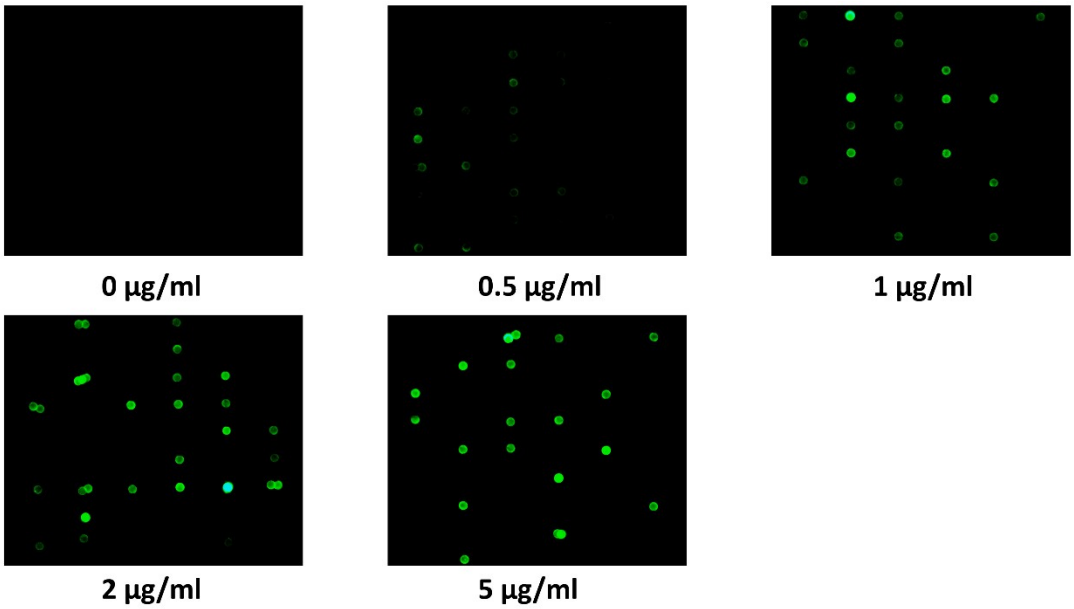

Figure S9. Fluorescence images of microbeads detecting different concentrations of anti-human IgG.